Macromolecular Research, Vol. 15, No. 4, pp 291-301 (2007)

Morphology and Rheology on the Blends of PLA/CMPS

Boo Young Shin, Gyu Soon Jo, Kyoung Su Kang, Tae Jin Lee, and Bong Shik Kim*

School of Display and Chemical Engineering, Yeungnam University, Gyeongsan 712-749, Korea

Sang Il Lee

Channel DM Co., Ltd., 12F, Gateway Tower, Seoul 140-709, Korea

Jeong Sup Song

Department of Chemistry, Sunmoon University, Chungnam 336-709, Koeea

Received November 6, 2006; Revised March 14, 2007

Abstract: The rheological behaviors and morphologies of polylactide (PLA) and chemically modified plasticized starch (CMPS) blends were investigated. For this study, oscillatory shear flow measurements of the PLA, CMPS and their blends were performed. A scanning electron microscope (SEM) study was also conducted on the extracted extrudates of the blends. The morphology of the blend changed in relation to the composition: sphere-shaped CMPS disperse/continuous PLA, rod-like deformed CMPS phase/continuous PLA, a co-continuous structure with bridged CMPS long rods and PLA dispersed/continuous CMPS. The composition of the phase inversion could be estimated and closely coincided from the observed morphology experimental results. The rheological behavior of the blends, from oscillatory measurements, was found to vary in relation to the composition, and reflected the morphologies of the blends. PLA showed Newtonian flow behavior, while CMPS showed strong shear thinning behavior. The relationships between the morphology and rheological properties were observed in detail.

Keywords: polylactide, plasticized starch, rheology, morphology.

Introduction

In recent years, the blend of polylactide (PLA) and granule starch were studied by many researchers because it will become more environmental and ecologically sound polymer and give economical benefit and combined property.[1-13] More recently, the development of thermoplastic starch (TPS) from granular starch and plasticizers provided a renewable, biodegradable and cost effective material flowable like other conventional thermoplastics.[14-16] Like most studies on polymer blends, to obtain desirable properties of blends the efforts of increasing interfacial adhesion between PLA and starch or TPS were made by many researchers.[5-13,17-19] There were many outcomes for good mechanical properties of PLA blends or composites but few studies on the understanding of rheological and morphological properties.

It is well known that the final morphology, which may occur during melt mixing, affects the blend properties and in turn on the application and also is highly affected by the melt rheological properties. Thus, understanding the melt rheological properties and morphology of blend is not only important in gaining fundamental knowledge of the processability and blend properties, but is also helpful in understanding the morphology-rheology-property relationships for the final stage of PLA blend.[20-26]

In this study we will observe the dynamic rheological properties and the changes of morphologies with chemically modified plasticized starch (CMPS) content by etching the extrudates of blends. In addition, the effects of composition on the rheological behavior in dynamic shear condition will be investigated in detail in connection with the blends morphologies.

Experimental

Materials. Poly(lactic acid) (NatureWork® PLA Polymer 2002D) with specific gravity of 1.24 and a melt flow index of 4-8 g/10 min (measured at 190 °C under a load 2.16 kg) was obtained from Cargill Dow LLC. Corn starch (11% inherent moisture) was obtained from Shindongbang Inc. Korea. It was used as purchased. Glycerol, sodium hydroxide and chloroform obtained from Ducksan Pure Chemical Co. Ltd, were used as purchased. 2,5-bis((tert-butylperoxy)

*Corresponding Author. E-mail: kimbs@ynu.ac.kr

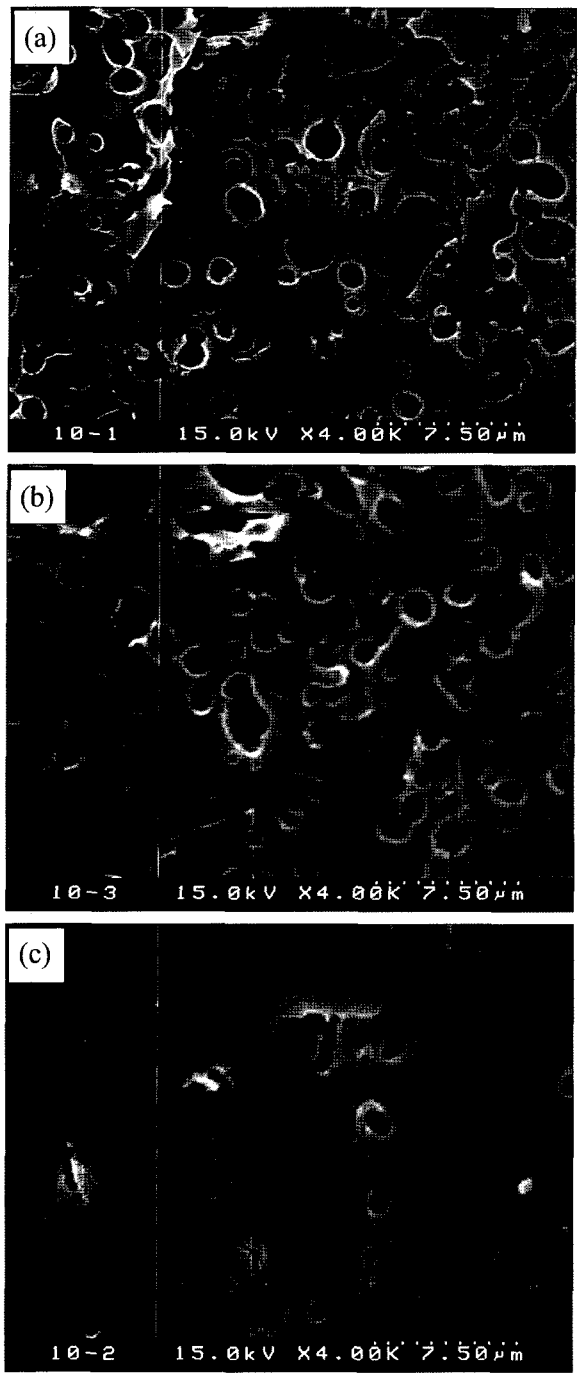

Figure 1. SEM images of the PLA phase after extraction of CMPS from the extrudate of CMPS10: fractured surface latitudinally (a), longitudinally (b) to the flow direction, and skin (c).

-2,5-dimethyl hexane (Luperox) and maleic anhydride (MA) were provided by Aldrich.

Preparing Chemically Modified Plasticized Starch. Starch was reactively modified using MA and plasticized using glycerol as the plasticizer in a twin-screw co-rotating extruder TEK45 (SM PLATEK Co.Ltd. Korea). The screw diameter was 46.2 mm with an *L/D* ratio of 30. The extruder was operated at 150 rpm. MA was grounded to a fine powder using a mortar and pestle and mixed with the starch using a tumbler blender for 15 min before being fed to the feed port of the extruder. Glycerol (GL) was mixed with Luperox and pumped to the extruder using peristaltic pump. The ratio of starch/GL was 8/2 by weight and the amount of MA and Luperox was 2 and 0.2 phr on basis of the total weight of starch and GL, respectively. A water vacuum was applied at the vent port to remove the unreacted MA and maleic acid (formed by reaction with water)/water mixture. The CMPS was collected and ground to a powder and stored in an aluminum laminated plastic bag.[18,19]

PLA/CMPS Blends. PLA and CMPS were blended in the ratios listed in Table I with twin-screw co-rotating compounding machine (SM PLATEK Co. Ltd., TEK 30, Korea). The screw diameter was 30 mm with an *L/D* ratio of 36. The extruder was operated at 150 rpm with a constant feed rate of 10 kg/h and barrel temperature range was 65-195 °C with die temperature 185 °C. The extruded strands were water quenched and then were cut to chips. The chips were dried in an oven for overnight at 50 °C. For ARES specimens, dried chips were compression molded to discs of 25 mm diameter and 2.5 mm thickness in a Carver laboratory hot press (Model 3851-O, Carver Inc.) at a set temperature 190 °C under 10 MPa.

Extraction Experiments. Solvent extraction has been used to visualize morphologies in a wide range of blends.[27-32] To observe the morphology of PLA/CMPS blends, we extracted each constituent by using carefully selected solvents. For this experiment we fractured frozen extrudate longitudinally and latitudinally in liquid nitrogen and then extracted in a selected solvent for 6 h at room temperature. In addition, chips of the blends were also extracted to observe the morphology of skin of extrudate. Sodium hydroxide (NaOH) solution (0.05 M) and chloroform were selected for dissolving CMPA and PLA, respectively.

Characterization. Measurements of rheological properties were performed using ARES (advanced rheometric expansion system; Rheometric Scientific Co. Ltd U.S.) with parallel-plate geometry. The equipment was run in the parallel plate configuration at a strain of 0.1% in frequency range of 0.1 to 100 rad/s at 190 and 200 °C. The morphologies of fractured surfaces of the extrudates were investigated by using scanning electron microscope (SEM; Hitachi model s-4100; Japan). The samples were coated with gold particles prior to the experiment.

Results and Discussion

Morphological Observation. It is well known that morphologies of immiscible blends are divided into four major types: dispersed particle-matrix structure, matrix-fiber structure, lamellar structures and co-continuous structures.[22] In

Table I. Composition, Power-Law Indexes and the Values of $\eta_1/\eta_2 \times \phi_2/\phi_1$ of PLA/CMPS Blends

Sample	Composition wt%		$\eta_1/\eta_2 \times \phi_2/\phi_1$ ω = 100 rad/s, 190 °C	Power-law Index* at 190 °C	Power-law Index* at 200 °C
	PLA	CMPS	-	-	-
PurePLA	100	-	-	0.92	0.95
CMPS10	90	10	0.07	0.95	0.95
CMPS20	80	20	0.14	0.94	0.98
CMPS30	70	30	0.26	0.65	0.46
CMPS40	60	40	0.39	0.41	0.21
CMPS50	50	50	0.57	0.19	0.19
CMPS60	40	60	0.82	0.17	0.11
CMPS70	30	70	1.19	0.17	0.11
CMPS80	20	80	1.70	0.31	0.13
CMPS	-	100	-	0.23	0.12

Note: The densities of PLA and CMPS were 1.24 and 1.46 g/cm^3, respectively. η_1/η_2: complex viscosity ratio of PLA/CMPS at frequency of 100 rad/s, $\eta_1/\eta_2 = 0.7$, ϕ_1: volume fraction of PLA, ϕ_2: volume fraction of CMPS. *Power-law indexes were calculated between frequencies 1 and 10 rad/s.

addition, these morphologies are related to the rheological properties of blends and vise versa.[21,22,31] To observe the real morphology of melt processing as possible, we used cold water quenched extrudates of blends for morphology study.

Figure 1 shows SEM micrographs of CMPS10 after extraction CMPS. Thus, the holes and the visible parts represent the extracted CMPS droplets and the continuous structure of PLA, respectively. Figures 1(a) (latitudinally fractured surface of extrudate) and 1(b) (longitudinally fractured surface of extrudate) indicate that the type of morphology is dispersed particle-matrix structure, that is, dispersed CMPS sphere-shaped particles imbedded in a continuous PLA phase. CMPS particles have a large distribution of sizes from submicron to 2 μm. Also, this morphology shows relatively poor distribution of CMPS particles compared to that of compatibilized blend, which shows a finer dispersion phase and well distribution due to reduced interfacial tension by compatibilizer.[22-24] The morphological difference between longitudinal and latitudinal fracture is not discernible. This result is indicating that the particles of CMPS in the extrudate are almost spherical shape. Figure 1(c) (the skin of extrudate) shows that the number of holes is reduced compared to those inside of extrudate, which might be caused by the morphological anisotropy. In immiscible blend, morphological change sometimes occurs in processed articles with the position such as skin and core due to the large difference of viscosity between constituents, distribution of shear stress, processing condition and concentration.[25]

As shown in Figure 2, the morphology of CMPS20 is a typical morphology of compatibilized binary blend showing finer CMPS particles than CMPS10 and well distributed narrower particle size (ca.1 μm). In this blend, the morphology still shows no directional difference indicating spherical particle shape of CMPS while, coagulated particles exist in the skin of strand (Figure 3(c)). Here is also the morphological anisotropy with position like that of CMPA10.

The disposition of the morphology of 30% CMPS blend in Figure 3 is somewhat different from those of Figures 1 and 2. The particle size increased in latitudinally fractured surface as shown in Figure 2(a) and elongated particles are first shown in the longitudinally fractured surface as shown in Figures 3(b) and (c). The length/diameter (*L/D*) ratio of deformed particles is not large and they start to join. Also we can see particles on the skin of extrudate were more elongated than those inside due to the result of wall shear stress and quenching process.

The morphologies of CMPS40 and CMPS50 show a clear matrix-fiber (long rod like) morphology. It is clear that the particles of CMPS were elongated to the flow direction and it became rod shaped with large *L/D* ratio morphology. Figure 4(a) (latitudinally fractured surface of extrudate) indicates that the diameter of rod is ca. 2-4 μm and some of rods are joined indicating the beginning of co-continuous morphology. Figures 4(b) (longitudinally fractured surface of extrudate) and (c) (skin of extrudate) show the long rod-shaped (fiber-like) CMPS phase morphology, which is clearly depend on the position of the extrudate, that is, the rods exist on the skin have large *L/D* ratio compared to those in inside of extrudate because they were subject to the highest shear stress (wall shear stress) among positions in extrudate and cooled fast after extrusion. Figure 5 shows the increased rod diameter and many rods are joined each other indicating a progressed co-continuous morphology but they are not fully interlocked.

The samples of CMPS60 were extracted with both NaOH solution and chloroform to verify the co-continuous phase in the same manner. Nevertheless, all the samples extracted by NaOH solution could not be self-supported and we could

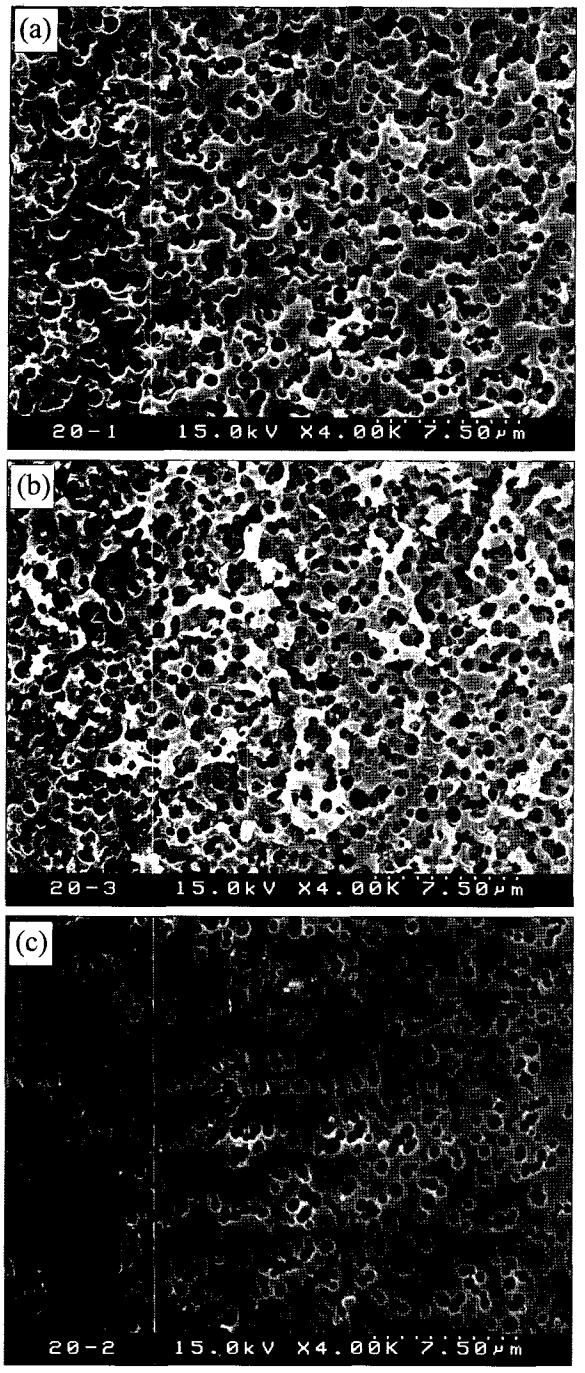

Figure 2. SEM images of the PLA phase after extraction of CMPS from the extrudate of CMPS20: fractured surface latitudinally (a), longitudinally (b) to the flow direction, and skin (c).

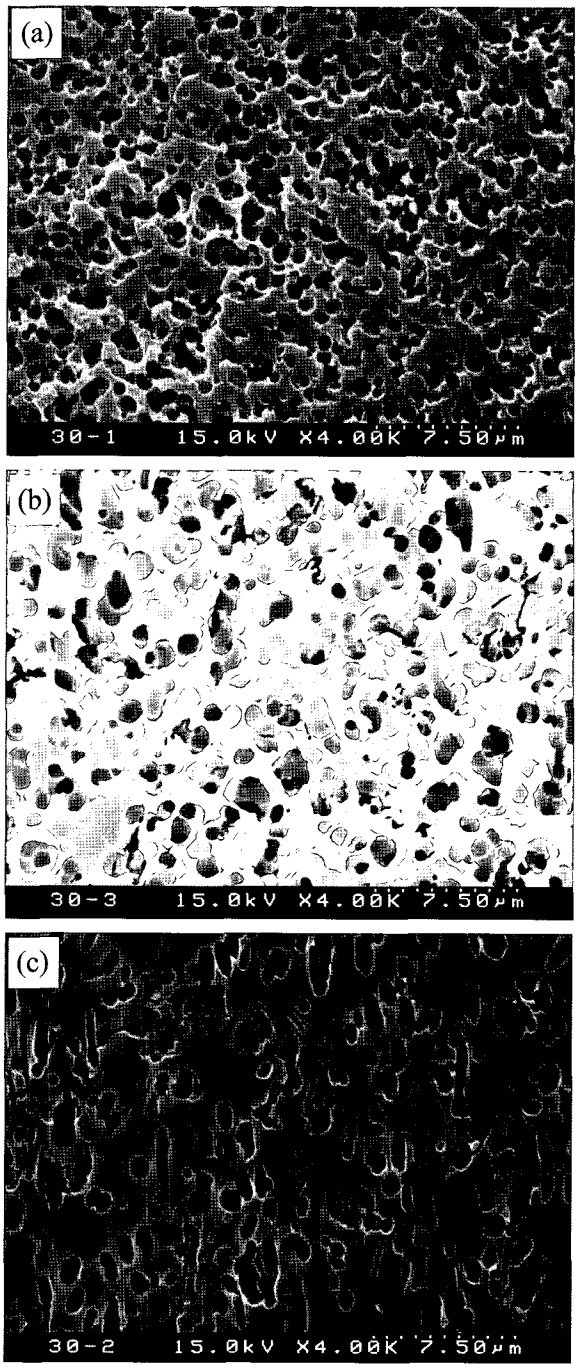

Figure 3. SEM images of the PLA phase after extraction of CMPS from the extrudate of CMPS30: fractured surface latitudinally (a), longitudinally (b) to the flow direction, and skin (c).

not identify the remains of PLA structure. On the other hand, the samples extracted by chloroform showed the collapsed structure of CMPA rods. As illustrated in Figure 6, the CMPS phase still keeps long rod shape with short branch. From these results we could imagine that the morphology of CMPS60 is fully co-continuous with well elongated and bridged CMPS phase. As shown in Figures 7 and 8 (extracted with chloroform), the holes and the visible parts represent the extracted PLA particles and the continuous structure of CMPS, respectively. This morphology shows the completion of phase inversion from CMPS disperse/PLA matrix morphology through co-continuous to PLA disperse/CMPS

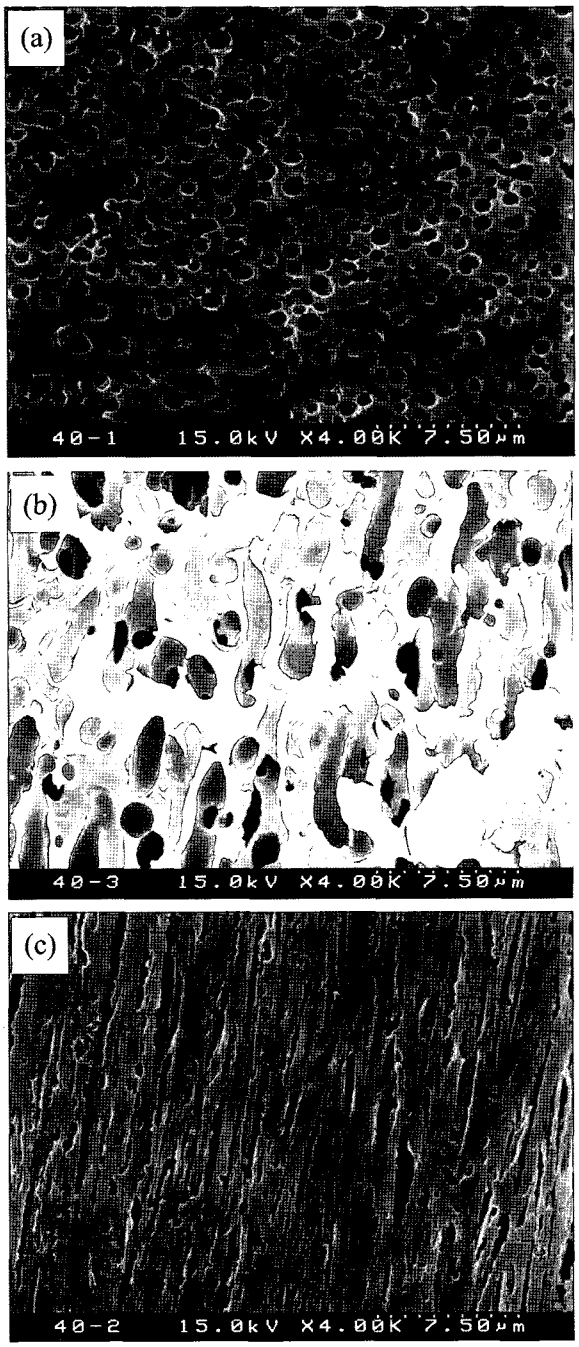

Figure 4. SEM images of the PLA phase after extraction of CMPS from the extrudate of CMPS40: fractured surface latitudinally (a), longitudinally (b) to the flow direction, and skin (c).

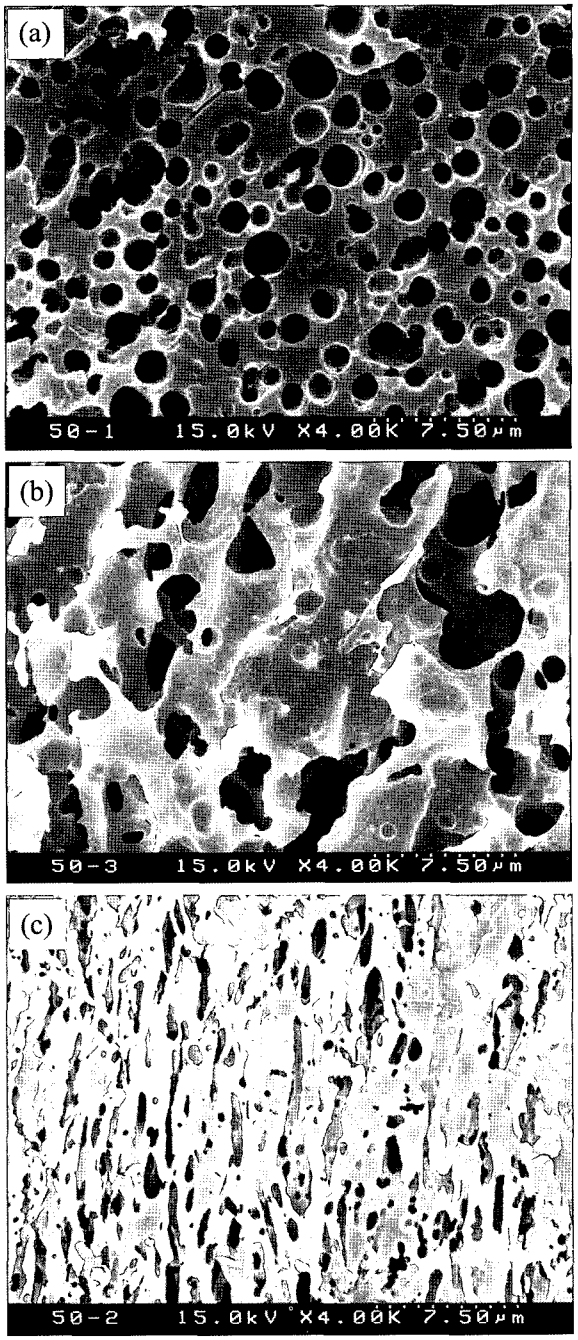

Figure 5. SEM images of the PLA phase after extraction of CMPS from the extrudate of CMPS50: fractured surface latitudinally (a), longitudinally (b) to the flow direction, and skin (c).

matrix. When we compared to the latitudinally fractured morphologies of CMPS30 in Figure 3(a), which has inversed composition CMPS70, the size of PLA particles is smaller than that of CMPS droplets in CMPS30 and there are seldom coagulated PLA particles. The longitudinally fractured surface (Figure 7(b)) shows some deformed particles but has low *L/D* ratio compared to those in Figure 3. Figure 8 shows very similar morphologies with CMPS70 but less deformed particles. We could not obtained useful morphology of the skin of extrudate due to the coarse surface.

We used Paul's[23,31,32] model to predict the phase-inversion composition. Assuming that the mean shear rate in the extrusion process was 100 s^{-1} and the Cox-Merz rule in relating the steady-shear viscosity with the absolute value of

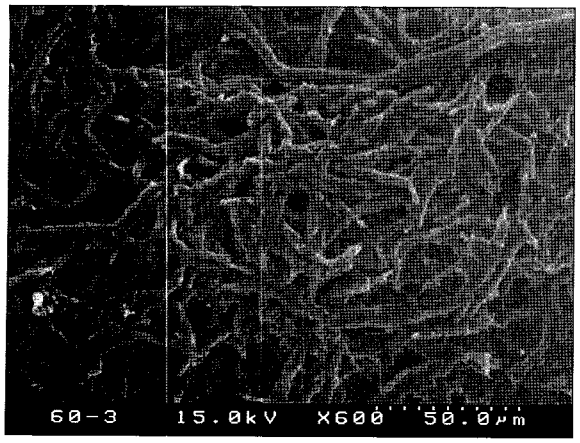

Figure 6. SEM images of the CMPS phase after extraction of PLA from the extrudate of CMPS60 fractured longitudinally to the flow direction.

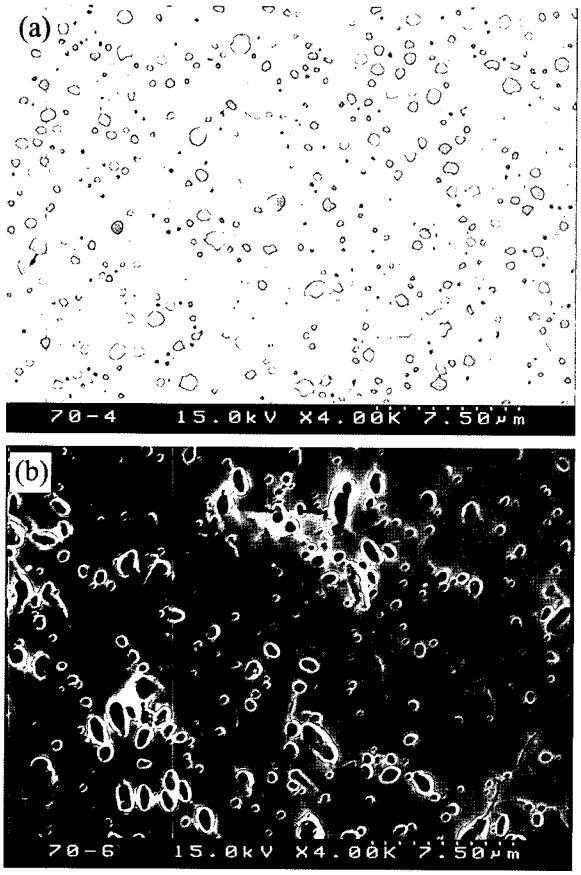

Figure 7. SEM images of the CMPS phase after extraction of PLA from the extrudate of CMPS70: fractured surface latitudinally (a) and longitudinally (b) to the flow direction.

the complex viscosity is valid, we used the complex viscosity values measured in frequency sweep at 100 rad/s to calculate viscosity ratio.[31,33] As listed in Table I, the estimated values of $\eta_1/\eta_2 \times \phi_2/\phi_1$ indicate that the composition of com-

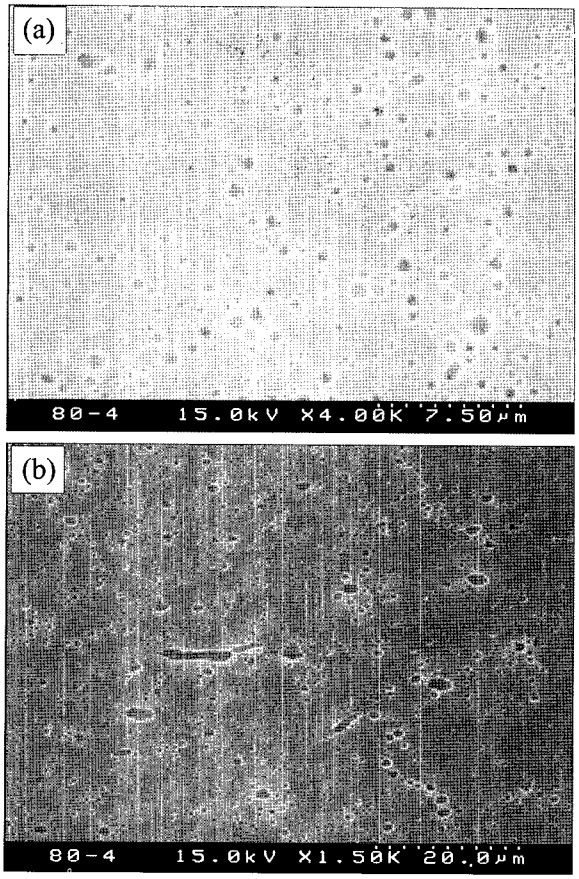

Figure 8. SEM images of the CMPS phase after extraction of PLA from the extrudate of CMPS80: fractured surface latitudinally (a) and longitudinally (b) to the flow direction.

plete co-continuous phase is about 65% of CMPS. In addition, the morphology CMPS70 is estimated as progressed co-continuous phase by the calculated value but the experimental morphology of CMPS70 showed completed phase inversion. This calculated CMPS compositions for phase inversion are slightly higher than that observed by SEM. Nevertheless, simple Paul's theory could approximately estimate the phase inversion composition for this blend system.

Rheological Study. Before starting dynamic frequency sweep tests, the linear viscoelastic range was determined through a strain sweep test. Storage modulus (G') and loss modulus (G'') were plotted as functions of strain% (γ). As shown in Figure 9, G' and G'' of PLA and CMPS remain constant to 10% and 1% of deformation showing the linear viscoelastic range, respectively. Following these results, we selected a deformation of 0.1% for all tests. Figure 10 depicts that PLA is a liquid-like fluid ($G'' > G'$) and CMPS is a solid-like fluid ($G' > G''$).

Figure 10 compares the complex viscosity versus the frequency for this blend system at 190 °C. PLA depicts a very long Newtonian viscosity plateau region while CMPS shows a pronounced shear-thinning flow behavior indicat-

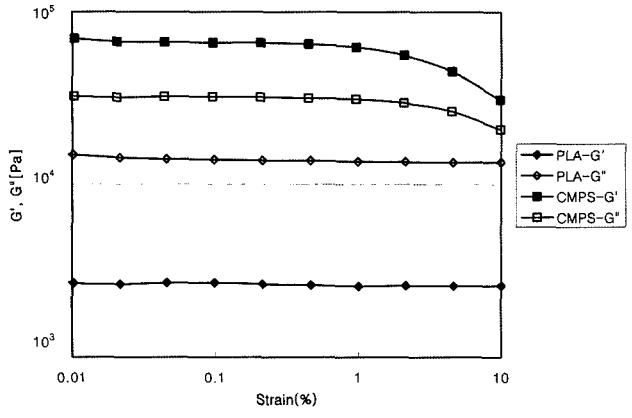

Figure 9. Curves of G' and G'' as a function of percent strain for PLA and CMPS at 190 °C.

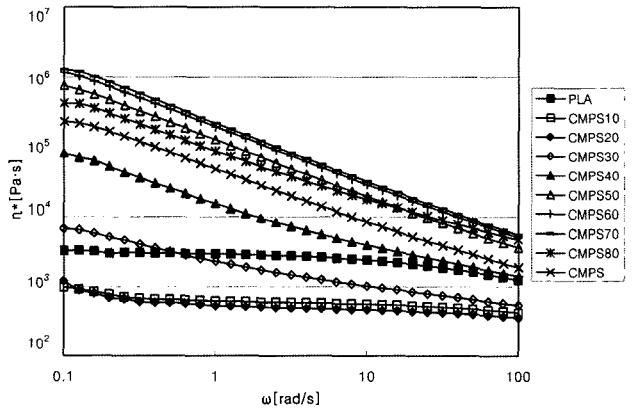

Figure 10. Curves of variation of complex viscosity (η^*) with angular frequency for the blend system of PLA and CMPS at 190 °C.

ing the tendency of easy molecular alignment tendency to the flow direction under shear stress. The complex viscosity of PLA is lower than that of CMPS within all the tested frequency range but the gab of viscosity difference decreased with increasing frequency due to the shear thinning behavior of CMPS. The flow behaviors of blends are also divided approximately into two typical categories: CMPS10 and CMPS20 show a Newtonian fluid like that of PLA and all the other blends show shear thinning flow behavior like that of CMPS. It is well known that power-law model is the most-used rheological equation for polymer. Of course, this model should be in reduced shear rate interval. The parameters of power-law model can be obtained by a simple redefinition of parameters[26]:

$$\eta = K_2 \dot{\gamma}^{n-1}$$

where n is called the power-law index and K_2 is called consistency. It is also known that there is analogous relation between dynamic and the steady shear data: complex viscosity (η^*) versus frequency (ω) and viscosity (η) versus shear rate ($\dot{\gamma}$) can be superimposed. The calculated power-law indexes of this blend system for the linear part of viscosity curve (frequency range from 1 to 10 rad/s) are listed in Table I. In general, the value of n for Newtonian fluid is 1.0, on the other hand that of pseudoplastic fluid is lower than 1.0. The more fluid shows pseudoplastic characteristic, the lower fluid has the value of power-law index. As listed in Table I, PLA and CMPS have power-law indexes of 0.92 and 0.23, respectively. CMPS10 and CMP20 have very similar power-law index values to that of PLA, while those of other blends decreases with increasing CMPS content. At over 50% CMPS the trend of power-law indexes is complicated, that is, CMPS50, CMPS60 and CMPS70 have lower power-law indexes but CMPS80 has higher value than that of pure CMPS. The results of lower and higher indexes of blends than that of CMPS might be illustrated by the morphology and diluent effect. As illustrated in morphology study, CMPS phases were long rod shapes and well oriented to the flow direction. Here, the addition moderate amount of low viscosity material of PLA could play a role as a diluent, which increases the sensitivity of the viscosity towards shear resulting in high shear thinning.[34] For the CMPS80, which has very small amount of PLA, the sphere-shaped dispersed droplets of PLA in matrix CMPS as shown in Figure 8 seemed to hinder the flow of CMPS matrix. Ziegler and Wolf[35] found that the extent of the shear thinning varies with the blend reflecting the morphology of blends in steady sear measurement. From the result of complex viscosity versus frequency and morphology of blends, we also could conclude that the extent of shear thinning measured in oscillatory measurement varies with composition reflecting the morphologies of blends.

Moreover, the complex viscosities of blends with frequency show very interesting results, that is, CMPS10 and CMPS20 have lower viscosities than those of main constituents of PLA and CMPS at any frequencies; CMPS30 has intermediate viscosity value between PLA and CMPS at low frequency, while, at high frequency it has lower values than those of PLA; CMPS40 has intermediate viscosity value between PLA and CMPS at any frequencies; over CMPS 50% blends have higher viscosities than those of both materials at any frequencies. In polymer blends, it is general trend that the values of viscosities of blends have intermediate values between those of both polymers.[22] At times there are exceptions, that is, blends have higher or lower rheological values than those of constituents and, what is more, there are crossover of rheological properties with shear rate or frequency between blends and constituents.[20-28,36] Anyway, this blend system has very complicated variation of complex viscosity values with composition and frequency.

Thus, we observed the composition effect on the complex viscosity of blend in detail. As shown in Figure 11, the complex viscosity-composition curves at constant frequencies of 0.1, 1, 10, and 100 rad/s show minimum and maximum

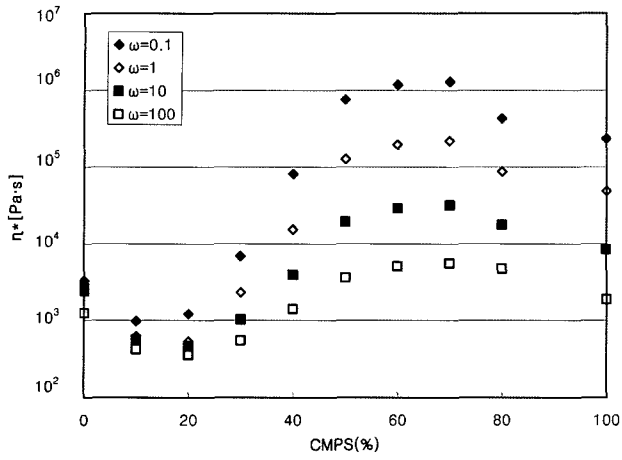

Figure 11. Composition dependence on complex viscosity at different frequencies for the blend system of PLA and CMPS at 190 °C.

complex viscosities at 20% and 70% CMPS, respectively. For the effect of composition on the viscosity, Han[37] summarized the viscosity-composition curves as four types: Type I, the viscosity decreases (or increases) monotonically with blend composition; Type II, the viscosity increases (or decreases), exhibiting an S shape; Type III, viscosity-composition curve goes through minimum; Type IV, viscosity-composition curve goes through maximum. Also, he tried to relate the bulk rheological behavior of two-phase polymer blends to their morphologies, that is, Type I occurs when the dispersed particles have relatively little interaction and the viscosity of dispersed phase is much greater than that of suspending medium (matrix polymer); Type II occurs when there is a phase inversion at a certain blending ratio and there is little attraction among dispersed particles; Type III occurs when the particles get sufficiently elongated, giving rise to thread-like fibrils that are aligned in the flow direction; Type IV occurs either when there are strong interactions among particles at low shear rates or when the blend has an interlocked morphology. More recently, Utraki[38] classified the blends system by the trend of rheological parameters-composition, that is, blend system can be divided into three classes by experimental data of rheological parameters (η, η_E, γ_r, N_1, G', G'') vs. composition: positive-deviation blend (PDB), negative-deviation blend (NDB), and positive-negative-deviation blend (PNDB). Where η is viscosity under steady shear, η_E elongational viscosity, γ_r strain recovery, N_1 first normal stress difference, G' storage modulus, and G'' loss modulus. Moreover, many researchers have tried to find the relationships between rheological properties and miscibility of blends by using these rheological properties-composition curves at constant shear rate (or frequency).[39-44] Though many researches discussed miscibility based on the experimental observation in terms of PCB, NDB, and PNDB, there are many exceptions.[39,40]

In this blend system, all the curves in Figure 11 show an S shape with minimum and maximum values with composition if we followed Han's classification. As discussed in morphological study, the morphologies of blend changed with the composition from CMPS dispersed/PLA matrix to co-continuous and finally went to phase inversion. For the interpretation of minimum viscosity at low CMPS composition (CMPS10 and CMPS20), we can imagine that morphological change of dispersed phase of CMPS under high shear stress, that is, the deformation of dispersed phase of CMPS aligned in the direction of flow.[37] As shown in Figure 10, pure CMPS has strong shear thinning behavior, which indicate the molecules are easily aligned to the flow direction. Though we could not obtain a valid evidence of the deformation of CMPS particles for these compositions from morphology as shown in Figures 1 and 2, we may assume that the morphological changes might occur during melt blending as follows: first, the dispersed/matrix morphology was induced at the end of barrel of the extruder during melt mixing, and then the dispersed particles of CMPS were elongated due to the high shear stress as they pass the narrow channel of the extruder die and finally elongated particles were recoiled to sphere-shaped particles after leaving the die. From these suggestions, the minimum viscosity at lower CMPS composition might be explained as the easy formation of elongated CMPS particles. The complex viscosities of CMPS30 and CMPS40 are approximately between those of PLA and CMPS due to the addition of high viscosity material, though these blends show a distinct thread like (long rod) morphology as shown in Figures 3(c), 4(b) and 4(c). Over CMPS 50% blends have higher viscosities than that of pure CMPS and maximum point at 70% CMPS content. The experimental observations of increased viscosity of blend were found in immiscible blends due to the decrease of free volume[36] or the interaction of dispersed droplets[37] and found in compatible or compatibilized blends.[18,23,24,36] As revealed in our previous study,[18,19] PLA/CMPS blends are compatible blend system due to the chemical bonds at the interface.

To observe the effect of temperature on the rheological properties, we plotted the complex viscosity-frequency curves and viscosity-composition curves obtained at 200 °C in Figures 12 and 13, respectively. As shown in Figure 12, the difference of complex viscosity between PLA and CMPS was reduced compared to the data observed at 190 °C. Moreover, at high frequency (100 rad/s) all the blends have lower complex viscosities than those of both constituents. The power-law indexes of most blends and pure CMPS decrease with increasing temperature but those of pure PLA, CMPS10, and CMPS20, which show Newtonian behavior, increased slightly as listed in Table I. Figure 13 depicts different complex viscosity-composition result at 200 °C. At 0.1 rad/s the curve is an S shape with minimum and maximum viscosities according to composition while,

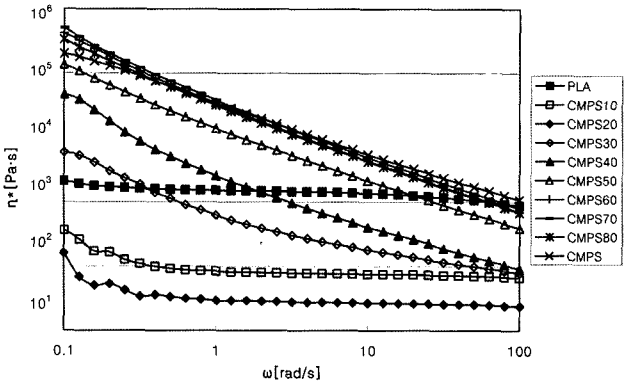

Figure 12. Curves of variation of complex viscosity with angular frequency for the blend system of PLA and CMPS at 200 °C.

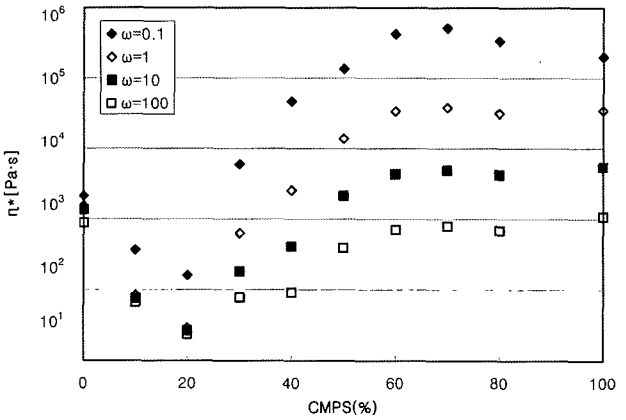

Figure 13. Composition dependence on complex viscosity at different frequencies for the blend system of PLA and CMPS at 200 °C.

at 1, 10, and 100 rad/s the curves show an S shape but do not have maximum point. Thus the change of viscosity-composition at elevated temperature may be caused by the change of viscosities resulting in morphological variation.[37]

If we classify the complex viscosity-composition curves by the way of Utraki,[38] Figure 11 exhibits a clear PNDB behavior from the log-additive rule for all frequencies, while Figure 13 shows PNDB and PND at low and high frequencies, respectively. From our previous research, it was concluded that this blend system is not miscible but compatible due to the reaction between CMPS and PLA.[18] Thus, to determine the miscibility of blend by this classification is not suitable at least for this blend system. As Utraki[38] mentioned in his article, there are low number of blends classified as PNDP and very confusing system, which could not be predicted and generalized.

The plot of modulus (G', G'') versus composition and logG' versus logG'' curve are shown in Figures 14-16. At low frequency from 0.1 to 1 rad/s, the G' values of PLA, CMPS10 and CMPS20 were too low to be used and were

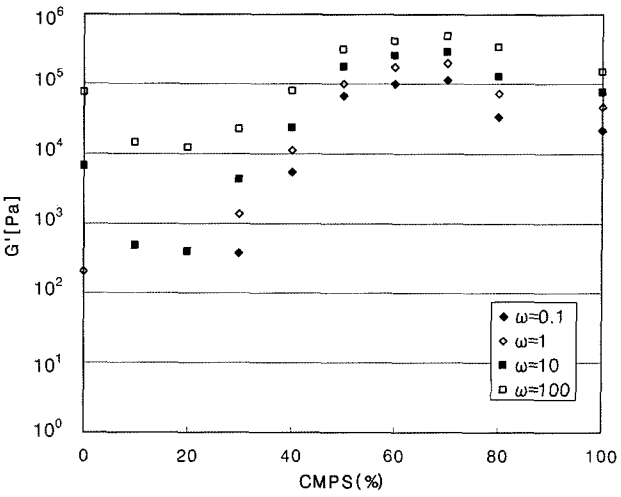

Figure 14. Composition dependence on storage modulus at different frequencies for the blend system of PLA and CMPS at 190 °C.

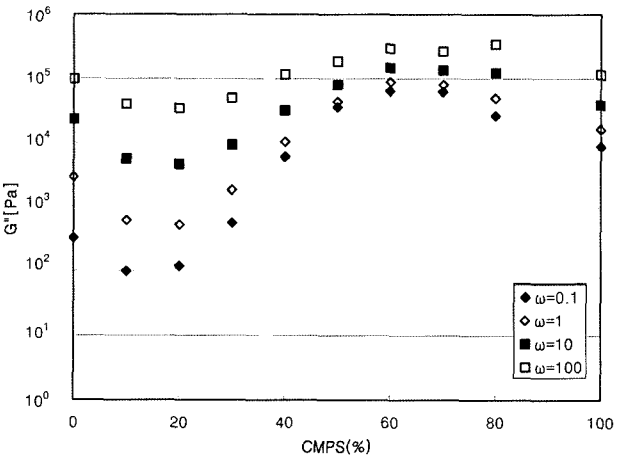

Figure 15. Composition dependence on loss modulus at different frequencies for the blend system of PLA and CMPS at 190 °C.

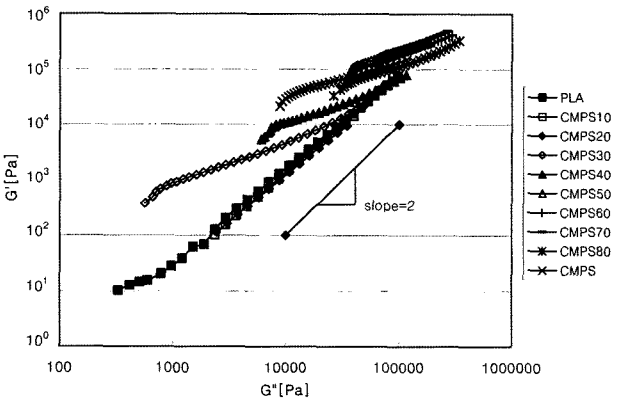

Figure 16. Plots of logG' versus logG'' for the blend system of PLA and CMPS at 190 °C.

much fluctuated due to the detecting limit of ARES. Thus we neglected the G' data below 100 Pa. Yang *et al.*[45] proposed the plot of logG'-logG'' to express the relative contribution of the G'' response to that of G''. Many researchers also tried to give a relationship between miscibility (or compatibility) and the plot of logG'-logG''.[23,39,45] In Figures 14 and 15, we could find that modulus-composition curves are S shape with minimum and maximum (or PNDB) like complex viscosity-composition curve. Meanwhile, the plots of logG'-logG'' (Figure 16) shows very similar trend to that of flow behavior of blend, that is, the plots of CMPS10 and CMPS20 fall on that of PLA, those of CMPS30 and CMPS40 lie between PLA and CMPS, other blends and CMPS show small extent of the spread among their plots. From these results, we might suggest that both properties of elastic and viscous properties of blends also mainly determined by the morphologies of blends induced during melt process.[37]

Conclusions

In this work, the dynamic rheological properties of blends of PLA and chemically modified plasticized starch were investigated in connection with their morphologies. We tried to get real morphologies of melt processing by observing the extrudate quenched by cold water in front of extruder die.

This blend system showed different morphologies with composition affected by shear stress during extrusion as follows: sphere-shaped CMPS disperse/PLA continuous at very low CMPS content and deformed CMPS particles with some *L/D* ratio/PLA continuous, which extended to complete co-continuous with long rods CMPS phase bridged each other with increasing CMPS content, and finally PLA dispersed/CMPS continuous morphology at very high CMPS content.

The flow behavior measured in dynamic shear, complex viscosity and storage modulus depended to a large extent on the composition in a characteristic manner reflecting the morphologies of blends. Pure PLA, CMPS10, and CMPS20 showed Newtonian fluid with power-law indexes around 0.95, while other blends and pure CMPS showed strong pseudoplastic fluid with those of 0.65-0.11, which depended on the composition. Complex viscosity and modulus-composition curves were PNDB behavior from the log-additive rule for all frequencies at 190 °C.

Acknowledgements. This work was supported by Eco-Technopia 21 project of Korea Institute of Environmental Science and Technology. The authors were supported from the second phase of BK21 program.

References

(1) R. Narayan, *National Institute for Standards and Technology*, September, 135 (1993).
(2) S. Bloembergaen, J. David, D. Geyer, A. Gustafson, J. Snook, and R. Narayan, in *Biodegradable Plastics and Polymers*, Y. Doi and K. Fukuda, eds., Elsvier, Osaka, 1993, pp 601-609.
(3) R. Narayan, *ACS Symposium*, **575**, 1 (1994).
(4) S. Jacobsen and H. G. Fritz, *Polym. Eng. Sci.*, **36**, 2799 (1996).
(5) J. W. Park and S. S. Im, *Polym. Eng. Sci.*, **40**, 2539 (2000).
(6) T. Ke and X. Sun, *J. Appl. Plym. Sci.*, **81**, 3069 (2001).
(7) H. Wang, X. Sun, and P. Seib, *J. Appl. Plym. Sci.*, **82**, 1761 (2001).
(8) H. Wang, X. Sun, and P. Seib, *J. Appl. Plym. Sci.*, **84**, 1257 (2002).
(9) T. Ke and X. Sun, *J. Appl. Plym. Sci.*, **88**, 2947 (2003).
(10) T. Ke and X. Sun, *J. Appl. Plym. Sci.*, **89**, 1203 (2003).
(11) H. Wang, X. Sun, and P. Seib, *J. Appl. Plym. Sci.*, **90**, 3683 (2003).
(12) J. F. Zhang and X. Sun, *J. Appl. Plym. Sci.*, **94**, 1697 (2004).
(13) J. F. Zhang and X. Sun, *Biomacromolecules*, **5**, 1446 (2004).
(14) W. Wiedmann and E. Strobel, *Starch*, **43**, 138 (1991).
(15) R. L. Shorgen, G. F. Fanta, and W. M. Doan, *Starch*, **45**, 276 (1993).
(16) L. Averous, L. Moro, P. Dole, and C. Fringant, *Polymer*, **41**, 4157 (2000).
(17) P. Dubois and R. Narayan, *Macromol. Symp.*, **198**, 233 (2003).
(18) B. Y. Shin, G. S. Jo, S. I. Lee, T. J. Lee, B. S. Kim, and R. Narayan, submitted (2006).
(19) R. Narayan, S. Blakrishnan, Y. Nabar, B. Y. Shin, P. Dubois, and J. M. Raquez, U.S. Patent 7, 153, 354 (2006).
(20) S. S. Ray and M. Okamoto, *Macromol. Rapid Commun.*, **24**, 815 (2003).
(21) C. D. Han and H. K. Chuang, in *Morphology of Polymers*, B. Sedlacek, ed., Walter de Gruyter & Co., New York, 1986, pp 103-118.
(22) H. V. Oene, in *Polymer Blends*, D. R. Paul and S. Newman, eds., Academic Press Inc., New York, 1978, pp 296-352.
(23) R. Krache, D. Benachour, and P. Pötschke, *J. Appl. Polym. Sci.*, **94**, 1976 (2004).
(24) S. H. Jafari, A. Yavari, A. Asadinezhad, H. A. Khonakdar, and F. Böhme, *Polymer*, **46**, 5082 (2005).
(25) L. C. Sawyer and D. T. Grubb, *Polymer Microscopy*, Champman and Hall Ltd., New York, 1987, pp 155-263.
(26) V. A. Alvarez, A. Terenzi, J. M. Kenny, and A. Vazquez, *Polym. Eng. Sci.*, **44**, 1907 (2004).
(27) M. Castro, C. Carrot, and F. Prochazka, *Polymer*, **45**, 4095 (2004).
(28) J. A. Galloway, K. J. Koester, B. J. Paasch, and C. W. Macosko, *Polymer*, **45**, 423 (2004).
(29) C. K. Kum, Y. T. Sung, M. S. Han, W. N. Kim, H. S. Lee, S. J. Lee, and J. Joo, *Macromol. Res.*, **14**, 456 (2006).
(30) H. M. Jeong, M. Y. Choi, and Y. T. Ahn, *Macromol. Res.*, **14**, 312 (2006).
(31) D. R. Paul and J. W. Barlow, *J. Macromol. Sci.-Rev. Macromol. Chem.*, **C18**, 109 (1980).
(32) S. Steinmann, W. Gronski, and C. Friedrich, *Polymer*, **42**, 6619 (2001).
(33) W. P. Cox and E. H. Merz, *J. Polym. Sci.*, **28**, 619 (1958).
(34) S. Steinmann, W. Gronski, and C. Friedrich, *Rheology Acta*, **41**, 77 (2002).

(35) V. Ziegler and B. A. Wolf, *J. Rheology*, **43**, 1033 (1999).
(36) H. J. Choi, S. H. Park, J. S. Yoon, and H. S. Lee, *Polym. Eng. Sci.*, **35**, 1636 (1995).
(37) C. D. Han, *Multi Phase Flow in Polymer Processing*, Academic Press Inc., New York, 1981.
(38) A. Utracki and M. R. Karmal, *Polym. Eng. Sci.*, **22**, 96 (1982).
(39) H. Kwang, D. Rana, K. Cho, J. Rhee, T. Woo, B. Lee, and S. Choe, *Polym. Eng. Sci.*, **40**, 2539 (2000).
(40) Y. Fang, P. J. Carreau, and G. Lafeur, *Polym. Eng. Sci.*, **45**, 1254 (2005).
(41) C. Liu, J. Wang, and J. He, *Polymer*, **43**, 3811 (2002).
(42) J. Y. Kim, S. W. Kang, S. H. Kim, B. C. Kim, K. B. Shim, and J. G. Lee, *Macromol. Res.*, **13**, 19 (2005).
(43) K. J. Hwang, J. W. Park, I. Kim, C. S. Ha, and G. H. Kim, *Macromol. Res.*, **14**, 179 (2006).
(44) J. U. Park, J. L. Kim, D. H. Kim, K. H. Ahn, S. J. Lee, and K. S. Cho, *Macromol. Res.*, **14**, 318 (2006).
(45) H. H. Yang, C. D. Han, and J. K Kim, *Polymer*, **35**, 1503 (1994).